中正嶺學報 第三十二卷 第一期 民國 92.11
JOURNAL OF C.C.I.T. VOL.32, NO.1, Nov. 2003

Linear Helicopter Model for Global Flight Envelope Control

Chi-Chung Luo*, Chien-Chung Kung, Po-Wei Chang*****
Ciann-Dong Yang*, and Yeong-Hwa Chang******

***Department of Electrical Engineering** **Department of Aeronautical Engineering**
Chung Cheng Institute of Technology, National Defense University
*****Institute of Aeronautics and Astronautics, National Cheng Kung University***
******Department of Electrica Engineering, Chang Gung University***

ABSTRACT

The goal of this paper is to set up a software-calculating helicopter dynamic, which can derive the linearized model from any trim point within the global flight envelope, so that we could afford nearly complete six degree-of-freedom model of a helicopter plant. We will establish the nonlinear and linear mathematical models of helicopter, which are the fundamentals of helicopter simulation and control. By using the principle of forces and moments equilibrium, we determine the trim points of different helicopter's flight conditions. At each trim point, the linearized model can be derived by Taylor’s series expansion. Our contributions will reduce the iteration numbers significantly and increase the modeling accuracy by proposed parallel trim procedure.

Keywords: helicopter linear model, nonlinear dynamic simulation, trim analysis

直昇機全空域線性模式的建立

羅其忠* 孔健君** 張伯偉*** 楊憲東*** 張永華****

*國防大學中正理工學院國防科學研究所 **國防大學中正理工學院航空系
***國立成功大學航空太空工程研究所 ****長庚大學電機系

摘要

本論文旨在建立直昇機動態的軟體模擬，可導出全空域飛行包絡中任一配平點的線性模式，以得到直昇機六自由度的完整模式；同時也建立了直昇機非線性及線性的數學模式做為控制模擬的基礎。利用力與矩的平衡原則，可決定直昇機各種飛行狀況的配平點，並在該配平點執行泰勒級數展開，以導出線性模式。本論文之貢獻在使用新提出的「平行配平步驟」，可大量減少迭代的運算時間及增加模式的準確度。

關鍵詞：直昇機線性模式、非線性動態模擬、配平分析

文稿收件日期 91.3.15；文稿修正後接受日期 92.6.17.
Manuscript received Mar. 15, 2002; revised June 17, 2003.

I. INTRODUCTION

This paper will make an integrated analysis and study in the helicopter relevant theories, including basic aerodynamics, control and maneuverability, etc. The very purpose is to derive a representation of a theoretical helicopter model via configuration data and aerodynamics, and to establish the nonlinear and linear helicopter mathematical models served as fundamentals of global flight envelope control and simulation under any control method. As for helicopter simulation, there exist four issues as following:

A. Modeling

Modeling issue is to establish the representation of forces and moments due to helicopter aerodynamics and to express the dynamic motion in a mathematical form as:

$$\dot{\mathbf{x}} = \mathbf{F}(\mathbf{x},\mathbf{u},t),\ \mathbf{x}(0) = \mathbf{x}_0 \qquad (1)$$

where $\mathbf{x}$ is system states, $\mathbf{u}$ is system control inputs, and $\mathbf{F}$ is a nonlinear vector function of $\mathbf{x}$ and $\mathbf{u}$.

B. Trim analysis

Finding the position of trim point $\mathbf{x}_e$ is to let net forces and moments summation be equal to zero (including aerodynamic, gravity and inertia force) under control $\mathbf{u}_e$. The mathematical manipulation is to solve $\mathbf{x}_e$ and $\mathbf{u}_e$ from the equation

$$\mathbf{F}(\mathbf{x}_e,\mathbf{u}_e)=0 \qquad (2)$$

C. Stability analysis

Stability analysis is to calculate the aerodynamic derivatives at the trim point $\mathbf{x}_e$ to get the linearized model, including system matrix $\mathbf{A}$ and control matrix $\mathbf{B}$, and to check the helicopter stability in the neighborhood of trim point, i.e. to solve the characteristic equation:

$$\det\left[\lambda\mathbf{I}-\left(\frac{\partial\mathbf{F}}{\partial\mathbf{x}}\right)_{\mathbf{x}_e}\right]=0 \qquad (3)$$

and verify whether the characteristic values λ's locate within the left-half s-plane or not.

D. Response analysis

Given control command $\mathbf{u}(t)$, response analysis is to find state response $\mathbf{x}(t)$. Its numerical integral solution can be solved as following.

$$\mathbf{x}(t)=\mathbf{x}(0)+\int_0^t \mathbf{F}(\mathbf{x}(\tau),\mathbf{u}(\tau),\tau)d\tau \qquad (4)$$

Section II to V are the theoretical kernels of helicopter's 4 issues mentioned above. Section II discusses the mathematical establishment of nonlinear helicopter model, and section III focuses on trim analysis and stability analysis. After getting the trim point at each flight condition, we derive the helicopter linear model just at that trim point. Section IV is concerned with the response analysis, and explains how to get dynamic responses. Section V contains a real example with given *Westland Lynx* helicopter data, and applies the theory mentioned above to derive helicopter models over global flight envelope.

II. NONLINEAR HELICOPTER MODEL

By using the theory of dynamics and aerodynamics, we will set up the mathematical representation of helicopter dynamic model in this section. A helicopter can be modeled as the combination of five interacting subsystems: mainrotor, fuselage, empennage, tailrotor and engine, as shown Fig.1. The resulting forces and moments of a flying helicopter come from the first four subsystems. As for each subsystem, we determine its degree of freedom in accordance with the simulation level and describe its behavior via dynamic equations. By combining aerodynamics of each subsystem, we can get the integrated helicopter dynamic equations [1,2].

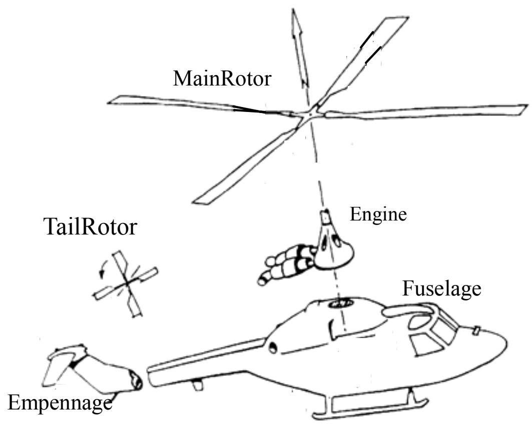

Fig.1. Five subsystems of helicopter.

For each subsystem, there are states to describe its behavior (assuming mainrotor and tailrotor all with 4 blades) [3]:

1. Mainrotor：β_0 , β_{1c} , β_{1s}
2. Fuselage ：u , v , w , p , q , r , ψ , θ , ϕ
3. Engine ：Ω , Q_e , $\dot{Q}_e$
4. Inflow ：λ_0 , λ_{0_T}

The six degree-of-freedom rigid body motion of helicopter can be described as following [4-7]:

A. Force equations

$$m_S\dot{U}=m_S\left(-WQ+VR\right)+F_X+d_X \tag{5a}$$

$$m_S\dot{V}=m_S\left(-UR+WP\right)+F_y+d_y \tag{5b}$$

$$m_S\dot{W}=m_S\left(-VP+UQ\right)+F_Z+d_Z \tag{5c}$$

B. Moment equation

$$I_{XX}\dot{P}=I_{XZ}\left(\dot{R}+PQ\right)+I_{Xy}\left(\dot{Q}-PR\right)-I_{yz}\left(R^2-Q^2\right)+\left(I_{yy}-I_{zz}\right)QR+L+d_l \tag{5d}$$

$$I_{yy}\dot{Q}=I_{xy}\left(\dot{P}+QR\right)+I_{zy}\left(\dot{R}-PQ\right)-I_{xz}\left(P^2-R^2\right)+\left(I_{zz}-I_{xx}\right)PR+M+d_m \tag{5e}$$

$$I_{zz}\dot{R}=I_{yz}\left(\dot{Q}+PR\right)+I_{xz}\left(\dot{P}-QR\right)-I_{yx}\left(Q^2-P^2\right)+\left(I_{xx}-I_{yy}\right)PQ+N+d_n \tag{5f}$$

C. Attitude equations

$$\dot{\phi}=p+\tan\theta\left(q\sin\phi+r\cos\phi\right) \tag{5g}$$

$$\dot{\theta}=q\cos\phi-r\sin\phi \tag{5h}$$

$$\dot{\psi}=\frac{q\sin\phi+r\cos\phi}{\cos\theta} \tag{5i}$$

where U, V, W, and P, Q, R are standard notations for linear and angular velocities, respectively, and all referred to the fuselage (body-fixed) axes system; I_{xx} , I_{xz} ,…, etc, are the moments of inertia of the helicopter; m_s is the helicopter's mass. Forces (F_x,F_y,F_z) and moments (L,M,N) include the effects coming from aerodynamics, gravity, and propulsion. They can be described as the sum of the contributions from the five subsystems

$$F_x=X_R+X_T+X_F+X_{tp}+X_{fn}-m_s g\sin\theta \tag{6a}$$

$$F_y=Y_R+Y_T+Y_F+Y_{tp}+Y_{fn}+m_s g\sin\phi\cos\theta \tag{6b}$$

$$F_z=Z_R+Z_T+Z_F+Z_{tp}+Z_{fn}+m_s g\cos\phi\cos\theta \tag{6c}$$

$$L=L_R+L_T+L_F+L_{tp}+L_{fn} \tag{6d}$$

$$M=M_R+M_T+M_F+M_{tp}+M_{fn} \tag{6e}$$

$$N=N_R+N_T+N_F+N_{tp}+N_{fn} \tag{6f}$$

where the subscripts stand for: rotor (R), tail rotor (T), fuselage (F), horizontal tail plane (tp), and vertical fin (fn). The orientation of fuselage is defined in terms of the Euler angles θ and ϕ with respect to an earth-fixed axes system. We substitute Eqs.(6) into Eqs.(5) and integrate to get the helicopter nonlinear dynamics.

III. LINEAR HELICOPTER MODEL

After constructing the helicopter nonlinear model, we recognize that actually the linearized model is more often used in designing control laws. Therefore how to get the linear model of helicopter is the most important work for control design. The procedures of linearization must start with the exact trim point, otherwise there will exist residual forces and moments which make the linearization unable to reflect the nonlinear character. So a trim condition (flight condition, or equilibrium point) must be set before getting the linear model, and then we take the Taylor's series expansion over this trim point to get the linear helicopter model. Linearization contains three procedures as following.

A. Assign flight conditions

The physical meaning of trim is to find the equilibrium point of helicopter motion, i.e. let all the derivatives be zero in the body-axis coordinate system. Note that the derivatives being zero in the body-axis coordinate system doesn't mean that the derivatives are zero in the inertia-axis coordinate system. Hence, there may still exist nonzero acceleration in the inertia-axis coordinate system, i.e. helicopter still can have the spin mode, as shown in Fig.2. By setting 4 trim parameters: flight velocity V_{fe}, flight path angle γ_{fe}, turn rate $\Omega_{ae}=\dot{\psi}$, and sideslip angle β_e, we can assign different flight conditions of helicopter. The fuselage velocity and angular velocity components at trim condition are expressed as

$$u=V_{fe}\left(\cos\chi_e\cos\gamma_{fe}\cos\theta-\sin\gamma_{fe}\sin\theta\right) \tag{7a}$$

$$v=V_{fe}[\sin\chi_e\cos\gamma_{fe}\cos\phi+\sin\phi(\cos\chi_e\cos\gamma_{fe}\sin\theta+\sin\gamma_{fe}\cos\theta)] \tag{7b}$$

$$w=V_{fe}[-\sin\chi_e\cos\gamma_{fe}\sin\phi+\cos\phi(\cos\chi_e\cos\gamma_{fe}\sin\theta+\sin\gamma_{fe}\cos\theta)] \tag{7c}$$

$$p=-\Omega_{ae}\sin\theta \tag{7d}$$

$$q=\Omega_{ae}\sin\phi\cos\theta \tag{7e}$$

$$r=\Omega_{ae}\cos\phi\cos\theta \tag{7f}$$

where χ_e is the artificial track angle which relates to the sideslip angle β_e.

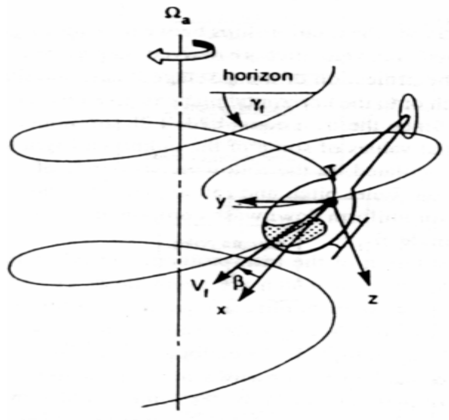

Fig.2. Assign flight conditions [4].

B. Parallel trim condition calculation

If we want to trim a nonlinear model, the derivatives in Eqs.(11) have to be zero. The entire trim algorithm can be divided into longitudinal trim, lateral/directional trim and main rotor speed trim. Before trimming a nonlinear model, we have to assign 4 flight condition parameters as well as initial guess values to those undetermined variables, and iterate those guess values repeatedly until the guess values converge to their steady-state values.

These initial-guess values include: β_0, β_{1c}, β_{1s}, θ, ϕ, θ_{0T} and Ω. The entire parallel trim processes are inflow iteration, longitudinal/ lateral trim and rotor speed trim, as shown in Fig.3.

Iteration method is to guess the initial values $\Theta_{initial}$ to calculate a newer Θ_{new}, and then compare the difference between them. If the difference is too large, then make another guess

$$\Theta_{new}=\Theta_{initial}+k_\Theta\left(\Theta_{new}-\Theta_{initial}\right)$$
$$\Theta_{initial}=\Theta_{new} \tag{8}$$

where k_Θ is a damping factor with value between 0 and 1, which means the iteration speed. The smaller k_Θ, and the iteration is more stable. k_Θ is set to 0.5 to iterate till the error is within the toleration range.

$$\left|\Theta_{new}-\Theta_{initial}\right|<\nu_\Theta\left|\Theta_{new}\right| \tag{9}$$

where ν_Θ is the relative tolerance coefficient. The inflow of mainrotor and tailrotor must be found in front of the parallel trim.

1. Iteration of mainrotor inflow

In high speed flight the rotor interacts with the air and induces the so-called inflow λ_i. The existence of inflow can affect the rotor aerodynamics heavily, so that the inflow effect must be considered. Normalizing velocities μ, μ_z and rotor thrust C_T in the usual way gives the general expression of rotor inflow λ_i as

$$\lambda_i\equiv\frac{C_T}{2\sqrt{\mu^2+\left(\lambda_i-\mu_z\right)^2}} \tag{10}$$

When $\lambda_i=\lambda_0$, we call λ_0 is the uniform inflow of mainrotor. C_T is given as

$$C_T\equiv\frac{T}{\rho\pi R^2\left(\Omega R\right)^2}=\frac{a_0 s}{2}\left(\begin{array}{l}\left(\frac{1}{3}+\frac{\mu^2}{2}\right)\theta_0+\frac{\mu}{2}\left(\theta_{1sw}+\frac{\bar{p}_{hw}}{2}\right)\\+\left(\frac{\mu_z-\lambda_0}{2}\right)+\left(\frac{1+\mu^2}{4}\right)\theta_{tw}\end{array}\right) \tag{11}$$

Since Eq.(5) is an nonlinear equation coupling Eq.(6), the iteration to solve inflow velocity is necessary. θ_{tw} and a_0 denote main rotor blade linear twist and lift curve slope.

The nonlinear equation Eq.(10) is iterated to get the inflow λ_0, the zero function is defined as

$$g_0=\lambda_0-\frac{C_T}{2\Lambda^{1/2}}\quad,\quad\Lambda=\mu^2+\left(\lambda_0-\mu_z\right)^2 \tag{12}$$

By means of Newton's iteration scheme, the newer value $\lambda_{0,i+1}$ of mainrotor inflow is as

$$\lambda_{0,i+1}=\lambda_{0i}+k_{\lambda 0}h_i\left(\lambda_{0i}\right) \tag{13}$$

where $k_{\lambda 0}$ is the damping factor and set to be 0.5 for a better convergent speed and stability.

$$h_i=-\frac{\left(2\lambda_{0i}\Lambda^{1/2}-C_T\right)\Lambda}{2\Lambda^{3/2}+a_0 s\Lambda/4-C_T\left(\mu_z-\lambda_{0i}\right)} \tag{14}$$

If the difference between the two inflow values is within the relative tolerance after iteration, then the mainrotor inflow velocity λ_0 and thruster coefficient C_T are found.

$$\left|\lambda_{0i}-\lambda_{0i-1}\right|<\nu_{\lambda 0}\left|\lambda_{0i}\right| \tag{15}$$

where $\nu_{\lambda 0}=10^{-10}$ is the relative tolerance coefficient. The same procedures are adopted to get the tailrotor inflow λ_{0T}

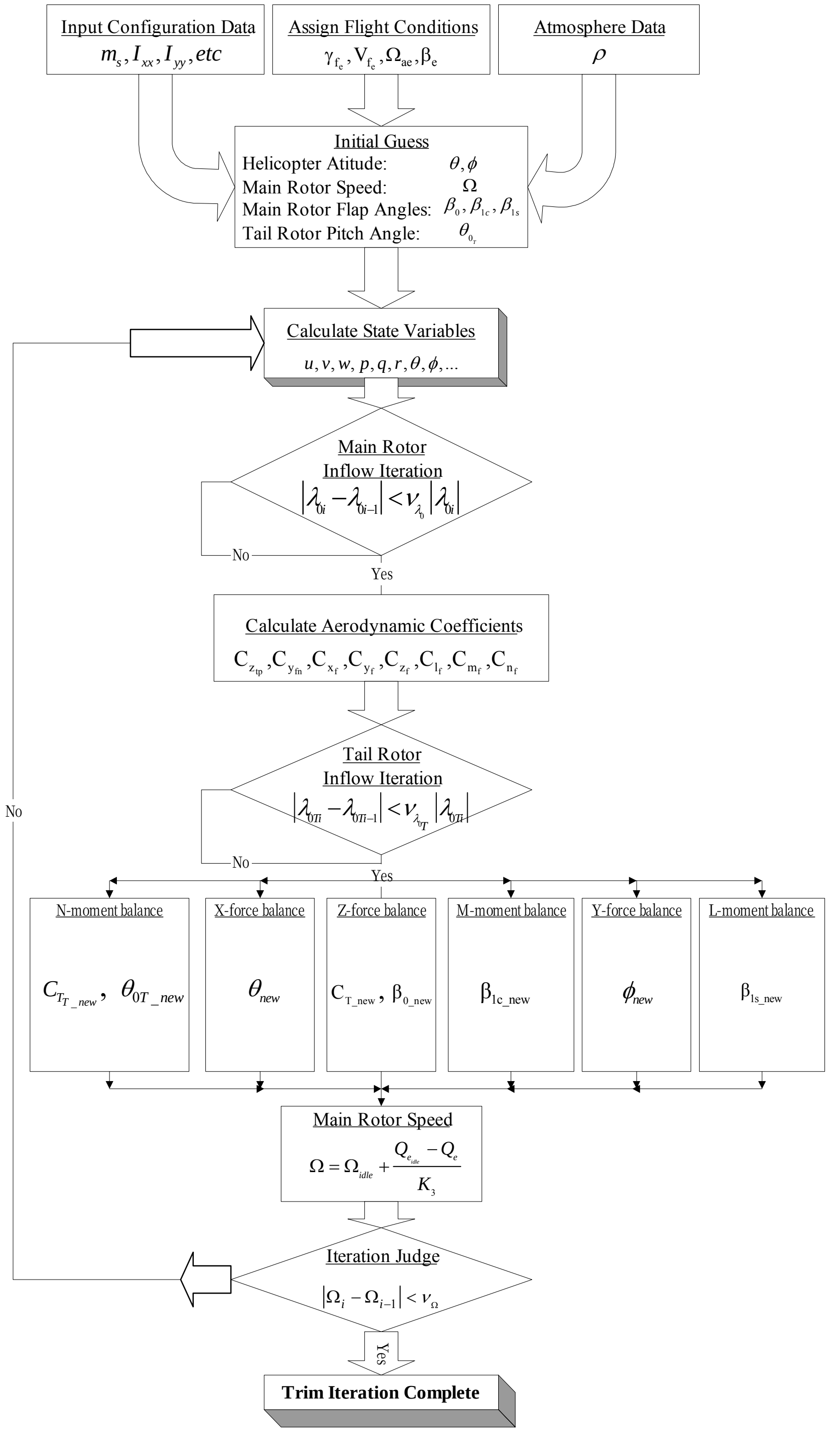

Fig.3. Iteration flow chart of parallel-trim analysis.

2. Iteration of parallel trim

There are enough variables to calculate the aerodynamic forces and moments until now, so we could start entering the trim iteration, which includes longitudinal trim and lateral/directional trim, and the absolute tolerance is induced to instead of the relative tolerance in [4].

a. Longitudinal trim to get new C_T and β_0

Considering the balanced force equation in z direction as

$$0=qu-pv+\frac{Z}{m_s}+g\cos\phi\cos\theta \qquad (16)$$

We find the z-direction acceleration and dimensionless acceleration as

$$a_z \equiv \frac{Z}{m_s}=pv-qu-g\cos\phi\cos\theta,\quad \overline{a}_z \equiv \frac{a_z}{\Omega^2 R} \qquad (17)$$

The aerodynamic forces of subsystems in Eq.(6) are expressed as following:

$$Z_R=X_h\sin\gamma_s+Z_h\cos\gamma_s \qquad (18)$$

$$X_h=X_{hw}\cos\psi_w-Y_{hw}\sin\psi_w,\ Y_h=X_{hw}\sin\psi_w+Y_{hw}\cos\psi_w,\ Z_h=Z_{hw} \qquad (19)$$

where

$$X_{hw}=\rho(\Omega R)^2\pi R^2 C_{xw},\ Y_{hw}=\rho(\Omega R)^2\pi R^2 C_{yw},\ Z_{hw}=\rho(\Omega R)^2\pi R^2 C_{zw} \qquad (20a)$$

$$C_{xw}=\tfrac{1}{2}\beta_{1cw}C_T+R_1,\quad C_{yw}=\tfrac{1}{2}\beta_{1sw}C_T+R_2,\quad C_{zw}=-C_T \qquad (20b)$$

The residual items R_i, i=1,2,3,4,5 are defined to get the thruster coefficient C_T, and the harmonic coefficients $F_0^{(1)}$, $F_{1s}^{(1)}$, $F_{1c}^{(1)}$, $F_{2c}^{(1)}$, $F_{2c}^{(1)}$, $F_{1c}^{(2)}$, $F_{1c}^{(2)}$ refer to [4].

$$R_1 \equiv \frac{a_0 s}{2}\left(\frac{F_{2c}^{(1)}}{4}\beta_{1cw}+\frac{F_{1c}^{(1)}}{2}\beta_0+\frac{F_{2s}^{(1)}}{4}\beta_{1sw}+\frac{F_{1s}^{(2)}}{2}\right) \qquad (21a)$$

$$R_2 \equiv \frac{a_0 s}{2}\left(\frac{F_{2c}^{(1)}}{4}\beta_{1sw}-\frac{F_{1s}^{(1)}}{2}\beta_0-\frac{F_{2s}^{(1)}}{4}\beta_{1cw}+\frac{F_{1c}^{(2)}}{2}\right) \qquad (21b)$$

The aerodynamic forces in z direction are summed up as

$$Z=Z_R+Z_T+Z_F+Z_{tp}+Z_{fn}=(X_h\sin\gamma_s+Z_h\cos\gamma_s)$$

$$+(-T_T\beta_{1swT})+(\frac{1}{2}\rho V_f^2 S_p C_{Zf})+(\frac{1}{2}\rho V_{tp}^2 S_{tp} C_{Ztp})+0 \qquad (22)$$

Eq.(18)~Eq.(22) are substituted into Eq.(17) to find the thruster coefficient as

$$C_T=\frac{1}{R_3}\left(\mu_1\overline{a}_z-R_4-R_5\right),\quad \mu_1=\frac{m_s}{\rho\pi R^3} \qquad (23)$$

where

$$R_3 \equiv \tfrac{1}{2}\beta_{1cw}\sin\gamma_s\cos\psi_w+\tfrac{1}{2}\beta_{1sw}\sin\gamma_s\sin\psi_w-\cos\gamma_s \qquad (24a)$$

$$R_4 \equiv R_1\sin\gamma_s\cos\psi_w-R_2\sin\gamma_s\sin\psi_w \qquad (24b)$$

$$R_5 \equiv -C_{TT}v_T\beta_{1swT}+\tfrac{1}{2}\left(\mu_f{}^2\overline{S}_p C_{zf}+\mu_{tp}{}^2\overline{S}_{tp}C_{ztp}\right) \qquad (24c)$$

$$v_T=g_T{}^2\left(\frac{R_T}{R}\right)^4,\ \overline{S}_p \equiv \frac{S_p}{\pi R^2},\ \overline{S}_{tp} \equiv \frac{S_{tp}}{\pi R^2} \qquad (25)$$

The new thruster coefficient induces a new collective pitch of mainrotor as

$$\theta_{0i}=\frac{1}{\frac{1}{3}+\frac{\mu^2}{2}}\left[\frac{2C_T}{a_0 s}-\frac{\mu}{2}\left(\theta_{1sw}+\frac{\overline{p}_{hw}}{2}\right)-\left(\frac{\mu_z-\lambda_0}{2}\right)-\left(\frac{1+\mu^2}{4}\right)\theta_{tw}\right] \qquad (26)$$

, and then a new collective flapping angle is as

$$\beta_{0i}=\frac{\gamma}{8\lambda_\beta^2}[\theta_0(1+\mu^2)+4\theta_{tw}(\frac{1}{5}+\frac{\mu^2}{6})+\frac{4}{3}\mu\theta_{1sw}$$

$$+\frac{4}{3}(\mu_Z-\lambda_0)+\frac{2}{3}\mu(\overline{p}_{hw}-\lambda_{1sw})] \qquad (27)$$

The new collective flapping angle β_{0i} replaces the old one, and continues to the next step without iteration. The same procedures are adopted in longitudinal trim to get a new longitudinal flapping angle β_{1c} and longitudinal trim to get a new pitch angle θ.

b. Lateral/directional trim to get new tailrotor thruster coefficient C_{TT} and collective pitch θ_{0T}

The balanced moment equation is as

$$0=\left(I_{xx}-I_{yy}\right)pq+I_{xz}qr+N \qquad (28)$$

The new tailrotor thruster coefficient is as

$$C_{TT}=\frac{R_{18}-R_{19}+R_{20}+R_{21}}{\left(\overline{l}_T+\overline{x}_{cg}\right)v_T} \qquad (29)$$

where the residual items are

$$R_{18} \equiv \tfrac{1}{2}\mu_f{}^2\overline{S}_s\left(\overline{l}_T C_{nf}-\overline{x}_{cg}C_{yf}\right)-\tfrac{1}{2}\mu_{fn}{}^2\overline{S}_{fn}\left(\overline{l}_{fn}+\overline{x}_{cg}\right)C_{yfn} \qquad (30a)$$

$$R_{19} \equiv \mu_1\left[\left(i_{yy}-i_{xx}\right)\overline{pq}+i_{xz}\overline{rq}\right] \qquad (30b)$$

$$R_{20} \equiv -m_\beta\beta_{1s}\sin\gamma_s+\left(\cos\gamma_s-\tfrac{1}{2}\beta_{1c}\sin\gamma_s\right)C_Q \qquad (30c)$$

$$R_{21} \equiv -\left(C_{xw}\sin\psi_w+C_{yw}\cos\psi_w\right)\overline{x}_{cg} \qquad (30d)$$

The new tailrotor thruster coefficient induces a new effective collective pitch of tailrotor as

$$\theta_{0T}^*=\frac{3}{1+\frac{3}{2}\mu_T{}^2}\left(\frac{2C_{TT}}{a_{0T}s_T}-\frac{\mu_{zT}-\lambda_{0T}}{2}-\frac{\mu_T}{2}\theta_{1swT}^*\right) \qquad (31)$$

, and derive a new collective pitch of tailrotor as

$$\theta_{0T,i}=\theta_{0T}^*\left[1-k_3\left(\frac{\gamma_T}{8\lambda_{\beta T}{}^2}\right)\left(1+\mu_T{}^2\right)\right]-k_3\left(\frac{\gamma_T}{8\lambda_{\beta T}{}^2}\right)\frac{4}{3}\left(\mu_{zT}-\lambda_{0T}\right) \qquad (32)$$

The new tailrotor collective pitch $\theta_{0T,i}$ replaces the old one, and continues to the next step without iteration. The same procedures are adopted in lateral/directional trim to get a new latitudinal flapping angle β_{1s} and lateral/directional trim to get new roll ϕ.

3. Mainrotor speed trim to get new rotor speed Ω

By using the droop law of powerplant, we derive the mainrotor speed as

$$\Omega=\Omega_{idle}-\left(Q_e-Q_{e_{idle}}\right)/K_3 \tag{33}$$

If the difference between the two mainrotor speed values is within the absolute tolerance ν_Ω after iteration, then the mainrotor speed $\Omega=\Omega_i$ is found, otherwise, repeat the whole trim procedure once again.

$$\left|\Omega_i-\Omega_{i-1}\right|<\nu_\Omega \tag{34}$$

where $\nu_\Omega=10^{-4}$ is the absolute tolerance coefficient.

C. Linearization

The linearization methodology utilizes Taylor's expansion at the trim point by using small perturbation theory, and keeping the linear terms to get the helicopter linear model [8,9]. A basic hypothesis is that the aerodynamic forces and moments are analytic functions of states, state derivatives and control surface angles. When Eqs.(11)~(12) are linearized, helicopter linear model cab be derived as

$$\dot{\mathbf{x}}=\mathbf{Ax}+\mathbf{Bu} \tag{35}$$

$$\mathbf{x}\equiv\left[u\ v\ w\ p\ q\ r\ \phi\ \theta\right]^T,\ \mathbf{u}\equiv\left[\theta_0\ \theta_{ls}\ \theta_{lc}\ \theta_{0T}\right]^T$$

where A is the helicopter system matrix, consisting of stability derivatives, which represent the characteristic of system. B is the control matrix consisting of control derivatives. Matrix A and B are shown in Fig.4.

IV. NONLINEAR SIMULATION

The nonlinear six degree-of-freedom (DOF_6) rigid-body equation of motion (EOM) Eqs.(11) are used to describe the motion of helicopter. Owing to those aerodynamic forces and moments being nonlinear functions of states and control surface angles, we call the model as 'nonlinear model'. We can obtain linear model by means of trimming and linearization for the purpose of stability analysis and control laws design. The linear model only describes the dynamic response of helicopter at the neighborhood of trim point; therefore it cannot describe the global response. Naturally we have to use nonlinear model for the sake of simulation fidelity. Although control laws are derived from linear mode, they must be put into the nonlinear model to verify the feasibility of linear control.

Besides Eqs.(4), the other states used in nonlinear simulation include:

A. Powerplant

$$\ddot{Q}_e=-\frac{1}{\tau_{e1}\tau_{e3}}[(\tau_{e1}+\tau_{e3})\dot{Q}_e+(Q_e-Q_{e_{idle}})+K_3(\Omega-\Omega_{idle}+\tau_{e2}\dot{\Omega})] \tag{36}$$

$$\dot{\Omega}=\dot{r}+\left(Q_e-Q_R-g_TQ_T\right)/I_R \tag{37}$$

B. Actuator

$$\begin{bmatrix}\dot{x}_0\\ \dot{x}_1\\ \dot{x}_2\\ \dot{x}_3\\ \dot{x}_4\end{bmatrix}=\begin{bmatrix}-0.02x_0+\theta_c\\ x_2\\ -19600x_1-196x_2+x_0\\ x_4\\ -4900x_3-98x_2+19600x_1\end{bmatrix} \tag{38}$$

$$\theta=4900x_3$$

Control surface movement is governed by actuator ability, and we take actuators used in UH-60 to be our actuator model. Given the initial states and control pitch angles, we can find the aerodynamic forces and moments at each simulation step. Substituting the forces and moments into the rigid-body DOF_6-EOM, we can find the present state derivative values, and then integrate those to get the state of next time step by Runge-Kutta method. The simulation process has 4 inputs (flight velocity V_{f_e}, flight path angle γ_{fe}, turn rate $\Omega_{ae}=\dot{\psi}$, sideslip angle β_e). Whenever the 4 flight condition parameters are assigned, all the aerodynamic derivatives, system matrix A and control matrix B can be found as will be shown in the next section.

V. SIMULATION EXAMPLE

Referring to the configuration data of *Westland Lynx* helicopter [4] and Jane's powerplant data [10], we can construct a helicopter model by numerical simulation. Taking level flight as an example, we can trim every flight condition to get the trim point at different flight velocity V_{fe}. This paper offers a new parallel-trim method to improve the sequential trim method proposed in [11], and makes a comparison with each other. For the lack of configuration data in [4], we estimate some other configuration data [5] to continue simulating.

We use MATLAB program to implement the level flight condition from 0m/s to 70m/s and do the trim analysis to get the trim point at every 5m/s intervals. The corresponding A and B matrices computed from Fig.4 for each trim point.

The state-derivative values should be zero theoretically, yet because of the trim algorithm convergence error and program round-off error, the calculated trim point is a little different from the real trim point. We can judge the trim effectiveness by the deviation of the state-derivative values from zero, and compare the simulation results with [11].

The maximal order of state-derivative values are within $O(10^{-5})$ as shown in Table.1. It's obvious that the maximal order of state derivative values is much smaller than that in Table.2 [11]. Our simulation results reveal that the trim results are reasonable and acceptable in linear model simulation. The robustness of the feedback controller designed later will overcome these linear modeling uncertainties.

When helicopter is in the hovering mode, the method proposed in [11] iterates 1359 times (runtime=92.49 sec for Pentium III-500Mhz CPU), and the maximal order of state derivative values is within $O(10^{-2})$ as shown in Fig.5(a), the horizontal axis represents the iteration number, and the vertical axis represents the value of the variable, but by our parallel-trim method shown in Fig.5(b) iterates only 19 times (runtime=2.8 sec for Pentium III-500Mhz CPU) and the maximal accuracy of state-derivative values is within $O(10^{-5})$. The iteration times are reduced significantly and the accuracy of state derivative values can increase three orders. In hovering mode, we find the linearized model whose system matrix eigenvalues are

$$-10.47,\ -1.96,\ -.287,\ -.261,\ -.000\pm .004i,\ .0543\pm .41i$$

where the real parts of a pair of conjugate complex roots are positive. It means that system is unstable at this trim point. If the configuration data of any kind of helicopter are given, our dynamic simulation program will calculate all the aerodynamic derivatives for that kind of helicopter. So does that of the Lynx helicopter, and the results are shown in Fig.6 and Fig.7 which indicate that the aerodynamic partial derivatives are varied with flight velocity V_{fe}.

Figure 8 is the helicopter free response with trim point as initial values, and its character of instability is predicted by the unstable eigenvalues of the linear model. We can design a simple state feedback controller for this linear model as

$$\mathbf{u} = -\mathbf{K}\mathbf{x} + \mathbf{r} \qquad (39)$$

where r is the reference command. By pole placement method, the poles of the close-loop system are chosen as

$$-10.47 \quad -2.12 \quad -2 \quad -3 \quad -2\pm 2i \quad -3\pm 3i$$

and the feedback gain matrix K is found to be:

$$\mathbf{A} = \begin{bmatrix} X'_u & X'_v + r & X'_w - q & X'_p & X'_q - w & X'_r + v & 0 & -g\cos\theta \\ Y'_u - r & Y'_v & Y'_w + p & Y'_p + w & Y'_q & Y'_r - u & g\cos\phi\cos\theta & -g\sin\phi\sin\theta \\ Z'_u + q & Z'_v - p & Z'_w & Z'_p - v & Z'_q + u & Z'_r & -g\sin\phi\cos\theta & -g\cos\phi\sin\theta \\ L'_u & L'_v & L'_w & L'_p + k_1 q & L'_q + k_1 p - k_2 r & L'_r - k_2 q & 0 & 0 \\ M'_u & M'_v & M'_w & M'_p - 2p\frac{I_{xz}}{I_{yy}} - r\frac{(I_{xx} - I_{zz})}{I_{yy}} & M'_q & M'_r + 2r\frac{I_{xz}}{I_{yy}} - p\frac{(I_{xx} - I_{zz})}{I_{yy}} & 0 & 0 \\ N'_u & N'_v & N'_w & N'_p - k_3 q & N'_q - k_1 r - k_3 p & N'_r - k_1 q & 0 & 0 \\ 0 & 0 & 0 & 1 & \sin\phi\tan\theta & \cos\phi\tan\theta & 0 & \Omega_{a_e}\sec\theta \\ 0 & 0 & 0 & 0 & \cos\phi & -\sin\phi & 0 & -\Omega_{a_e}\cos\theta \end{bmatrix}$$

$$\mathbf{B} = \begin{bmatrix} X'_{\theta_0} & X'_{\theta_{1s}} & X'_{\theta_{1c}} & X'_{\theta_{0T}} \\ Y'_{\theta_0} & Y'_{\theta_{1s}} & Y'_{\theta_{1c}} & Y'_{\theta_{0T}} \\ Z'_{\theta_0} & Z'_{\theta_{1s}} & Z'_{\theta_{1c}} & Z'_{\theta_{0T}} \\ L'_{\theta_0} & L'_{\theta_{1s}} & L'_{\theta_{1c}} & L'_{\theta_{0T}} \\ M'_{\theta_0} & M'_{\theta_{1s}} & M'_{\theta_{1c}} & M'_{\theta_{0T}} \\ N'_{\theta_0} & N'_{\theta_{1s}} & N'_{\theta_{1c}} & N'_{\theta_{0T}} \\ 0 & 0 & 0 & 0 \\ 0 & 0 & 0 & 0 \end{bmatrix}$$

Fig.4. Matrix A and B of linear helicopter model.

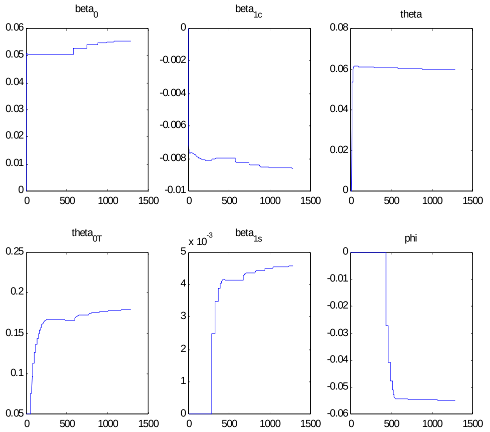

(a) serial trim.

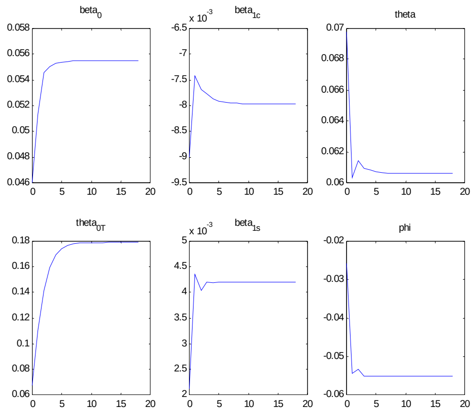

(b) parallel trim

Fig.5. Results of trim analysis for iteration variables $\beta_0, \beta_{1c}, \beta_{1s}, \phi, \theta, \theta_{0T}$.

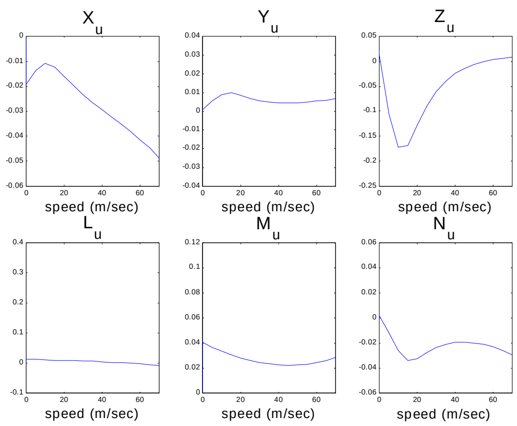

Fig.6. Aerodynamic partial derivative-u stable partial derivative.

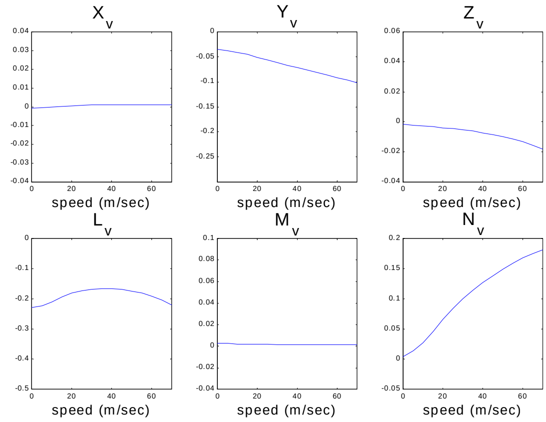

Fig.7. Aerodynamic partial derivative-v stable partial derivative.

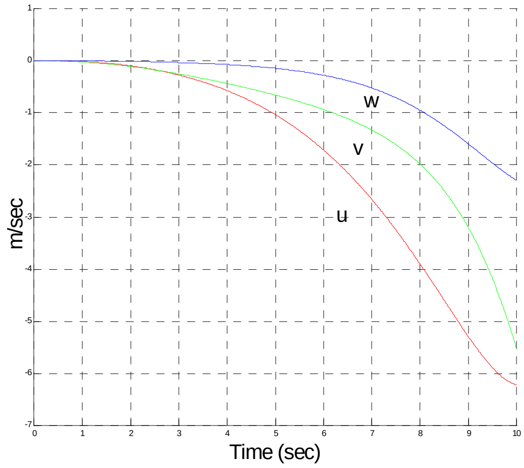

Fig.8. Open-loop free response with given initial values (Hovering).

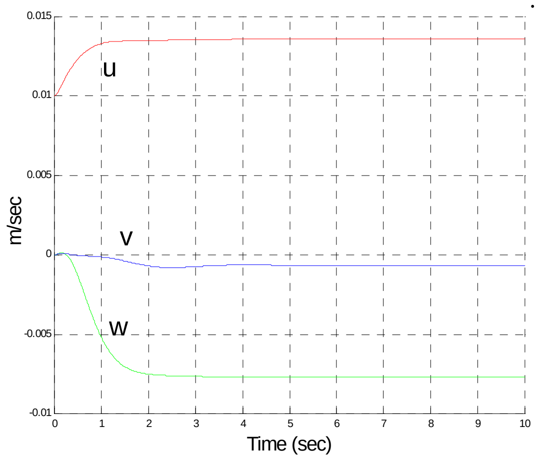

Fig.9. State feedback response with given initial values (Hovering).

$$K=\begin{bmatrix} 0.0019 & 0.0034 & -0.0306 & 0.0029 & -0.0005 & 0.0015 & 0.0185 & 0.0030 \\ -0.2847 & -0.0509 & -0.0181 & -0.0400 & 0.3182 & 0.0122 & -0.2263 & 1.6203 \\ 0.0388 & -0.0185 & -0.0006 & 0.0213 & -0.0237 & -0.0123 & -0.1657 & -0.2409 \\ 0.0757 & 0.0965 & -0.0287 & 0.0960 & -0.1110 & -0.1011 & 0.5543 & -0.4042 \end{bmatrix} \quad (40)$$

Setting the reference command r=0, we obtain Fig.9 as the nonlinear response after the controller is engaged. It's obvious that the designed control law can make system states stable in Fig.9, but the system steady-state values are a little away from the original trim points and reach to a new equilibrium position. This phenomenon is owing to numerical errors in trim calculation, and there still exist the residual forces and moments which are so-called uncertainties. When controller is to be designed, these uncertainties must be considered and overcome.

The controller design is not the key subject of this paper, but the establishment of global helicopter linear model, as shown in Appendix, is very precious and useful for the design of the linear control laws, since it's never afforded in the domestic or abroad documents. The matrix A and B in Appendix can serve as a database for the time-varying plant, so the readers can test them in any control theory that they are interested in, such as robust control, adaptive control, gain-scheduling control, etc.

VI. CONCLUSIONS

This paper is to establish helicopter linear mode for global flight envelope by means of only a set of detailed configuration data of helicopter. By inputting 4 flight conditions, we can compute the states, aerodynamic partial derivatives and

system characteristic A, B matrices of helicopter for any flight condition. When compared with [1], our iterative method converges more quickly and the state-derivatives at trim are more close to 0. The proposed method reduces the iteration numbers significantly and increases the modeling accuracy by using parallel-trim procedures. Finally, we make a comparison with the results in [1] to express our improvement in trim analysis and give the piecewise A and B matrices covering the global flight envelope for *Lynx* helicopter.

RRFERENCES

[1] Su, C. Z., “Constructing Helicopter Remote Control Testing System,” M.S. Thesis, National Cheng Kung University, Taiwan, 1997.

[2] Hong, C. C., “Helicopter Remote Control stabilized System Design and Implement,” M.S. Thesis, National Cheng Kung University, Taiwan, 1997.

[3] Padfield, G. D., Helicopter Flight Dynamics: The Theory and Application of Flying Qualities and Simulation Modeling, AIAA, 1996.

[4] Chou, D. W., “Modeling and Simulations of Helicopter Motions,” M.S. Thesis, National Cheng Kung University, Taiwan, 1998.

[5] Stevens, B. L. and Lewis, F. L., Aircraft Control and Simulation, John Wiley & Sono, New York 1992.

[6] Ginsberg, J. H., Advance Engineering Dynamics, Harper & Row, New York, 1988.

[7] Hohenemser, K. H. and Yin, Sheng-Kuang, “Some Applications of the Method of Multiblade Coordinates,” Journal of the American Helicopter Society, Vol. 17, No. 3, pp. 3-12, 1972.

[8] Newman, S., The Foundations of Helicopter Flight, London, Edward Arnold, 1994.

[9] Johnson, W., Helicopter Theory, Princeton University, New Jersey, 1980.

[10] Jane’s All The World’s Aircraft, 1995, Gili, P.A., and Battipede, M., “A MIMO Neutral Autopilot for a Nonlinear Helicopter Model,” AIAA Guidance, Navigation and Control Conf., Portland, OR, Aug. 1999.

[11] Chou, D. W. and Yang, C. D., "Constructing Helicopter Dynamic Simulation", Transactions of the Aeronautical and Astronautical Society of the Republic of China, Vol.32, No.3, pp.21-31, 2000.

NOMENCLATURE

a_0	main rotor blade lift curve slope (1/rad)
C_Q, C_{QT}	mainrotor/tailrotor torque coefficient
C_T, C_{TT}	rotor/tailrotor thrust coefficient
C_x, C_y, C_z	main rotor x, y, z-axis force coefficients
$\beta_0, \beta_{1c}, \beta_{1s}$	blade coning, longitudinal, lateral flapping angles
p,q,r	deviations of roll, pitch, yaw rate
u,v,w	deviations of forward, sideward, downward speed
Q_e	engine torque (N m)
Q_R, Q_T	main and tail rotor torque (N m)
R, R_T	main and tail rotor radius (m)
s, s_T	rotor/tailrotor solidity

γ_s shaft angle (rad)

μ, μ_z advance ratio, velocities of the rotor hub

ϕ, θ, Ψ Euler angles (rad)

θ_0, θ_{0T} main and tail rotor collective pitch angle

θ_{1s}, θ_{1c} longitudinal and lateral cyclic pitch

θ_{tw} main rotor blade linear twist (rad/m)

Ω, Ω_T main and tail rotor speed (rad/s)

S_p, S_s, S_{tp} fuselage top-view, side-view, tail plane area (m^2)

l_F fuselage reference length (m)

l_{fn}, l_{tp} distance of fin / tp c.p. of ref.point along negative *x*

h_R height of main rotor hub above fuselage reference point

h_T height of tail rotor hub above fuselage reference point

Subscript:

w, hw hub/wind-axis coordinate system
h hub coordinate system
b blade coordinate system
f fuselage (body-axis) coordinate system
R, T, F, fin, tp main rotor, tail rotor, fuselage, fin, tailplane
1c, 1s :sin/cos function expansion's 1st -order harmonic term

Table.1. The state derivative values of parallel trim results (main rotor speed is fixed), Absolute tolerance $\nu_\Omega = 10^{-4}$.

Flight Velocity (m/sec)	$\dot{u}$	$\dot{v}$	$\dot{w}$	$\dot{p}$	$\dot{q}$	$\dot{r}$
0	-1.1971 e-7	-2.0574 e-6	1.7804 e-6	4.6799 e-7	-1.7761 e-7	5.4867 e-6
5	-1.5892 e-7	-2.75628 e-6	2.1405 e-6	6.4135 e-7	-1.8156 e-7	7.38304 e-6
10	-2.4069 e-7	-5.2292 e-6	2.9797 e-6	1.2277 e-6	-2.341 e-7	1.4119 e-5
20	-8.2166 e-7	-3.0569 e-5	8.7225 e-6	7.0990 e-6	-5.6071 e-7	8.3233 e-5
30	-7.1645 e-7	-2.5424 e-5	6.3915 e-6	5.9061 e-6	2.5253 e-8	6.9248 e-5
40	-1.7212 e-7	-8.8812 e-6	1.1836 e-6	1.2391 e-6	-5.4261 e-7	2.4092 e-5
50	1.3042 e-6	-1.4085 e-6	-1.2225 e-5	-1.1632 e-5	-1.2344 e-5	3.0711 e-6
60	5.7613 e-7	4.1339 e-7	-4.7297 e-6	-3.7533 e-6	-4.8042 e-6	-1.173 e-6
70	-2.4878 e-6	-2.4589 e-6	7.4573 e-6	-1.9098 e-5	-2.1917 e-5	9.9821 e-7

Table.2. The state derivative values of serial trim results (main rotor speed is fixed), Relative tolerance $\nu_\Omega = 10^{-4}$

Flight Velocity (m/sec)	$\dot{u}$	$\dot{v}$	$\dot{w}$	$\dot{p}$	$\dot{q}$	$\dot{r}$
0	-6.6642 e-5	-8.1344 e-5	1.1099 e-3	-5.6431 e-2	1.8357 e-2	-1.0126 e-2
10	-9.8527 e-5	-9.6940 e-5	1.4857 e-3	-3.8298 e-2	1.5181 e-2	-6.8599 e-3
20	-6.1351 e-5	-5.2971 e-5	8.5128 e-4	-1.7834 e-2	1.1705 e-2	-3.1786 e-3
30	-9.9480 e-5	-5.0397 e-5	1.3361 e-3	-1.0330 e-2	1.0922 e-2	-1.8654 e-3
40	-1.0552 e-4	-3.7756 e-5	1.3915 e-3	-8.7373 e-3	1.1906 e-2	-1.6034 e-3
50	-1.3890 e-4	-2.9453 e-5	1.7973 e-3	-1.0587 e-2	1.3421 e-2	-1.9924 e-3
60	-1.1151 e-4	-2.8591 e-5	1.3519 e-3	-1.6528 e-2	1.2179 e-2	-3.0335 e-3
70	-2.1174 e-4	-3.8572 e-5	2.2861 e-3	-2.7950 e-2	-1.0467 e-3	-5.1953 e-3

APPENDIX

A, B matrices of *Lynx* helicopter linear model

1. Flight conditions: fly forward from (hovering) u=0 m/s to u=70m/s
2. Every 5m/s interval trim once
3. A_0 means A matrix at flight velocity u=0m/s, A_5 means u=5m/s

$$\mathbf{A}_0 = \begin{bmatrix} -0.0191 & -0.0008 & 0.0172 & -0.3371 & 0.3840 & 0 & 0 & -9.7920 \\ 0.0010 & -0.0349 & -0.0015 & -0.4032 & -0.3381 & 0.1168 & 9.7771 & 0.0328 \\ 0.0141 & -0.0015 & -0.2994 & -0.0256 & 0.0231 & -0.0000 & 0.5406 & 0.5930 \\ 0.0130 & -0.2290 & 0.0003 & -10.6200 & -3.0471 & -0.0333 & 0 & 0 \\ 0.0405 & 0.0024 & -0.0027 & 0.5281 & -1.8394 & -0.0015 & 0 & 0 \\ 0.0020 & 0.0039 & 0.0061 & -1.8554 & -0.5412 & -0.3487 & 0 & 0 \\ 0 & 0 & 0 & 1.0000 & -0.0033 & 0.0606 & 0 & 0 \\ 0 & 0 & 0 & 0 & 0.9985 & 0.0552 & 0 & 0 \end{bmatrix}$$

$$\mathbf{B}_0 = \begin{bmatrix} 5.3046 & -10.3467 & 1.0795 & 0 \\ -0.3565 & -1.0821 & -10.3723 & 4.7240 \\ -87.0074 & -0.7294 & 0.0755 & 0 \\ 7.5472 & -27.2884 & -156.4450 & -1.0690 \\ -1.5292 & 27.0904 & -4.7238 & -0.1858 \\ 17.7461 & -4.8969 & -27.9732 & -12.9307 \\ 0 & 0 & 0 & 0 \\ 0 & 0 & 0 & 0 \end{bmatrix}$$

$$\mathbf{A}_{25} = \begin{bmatrix} -0.0199 & 0.0009 & 0.0309 & -0.2566 & -0.4320 & 0.0000 & 0 & -9.8026 \\ 0.0068 & -0.0566 & -0.0077 & 0.3749 & -0.2551 & -24.6561 & 9.7982 & 0.0114 \\ -0.0891 & -0.0046 & -0.6355 & -0.2546 & 25.0298 & -0.0001 & 0.2946 & -0.3798 \\ 0.0074 & -0.1729 & 0.0116 & -10.6628 & -2.6214 & -0.0483 & 0 & 0 \\ 0.0262 & 0.0017 & -0.0250 & 0.4728 & -2.1380 & -0.0004 & 0 & 0 \\ -0.0274 & 0.0840 & -0.0225 & -1.8156 & -0.3324 & -0.8800 & 0 & 0 \\ 0 & 0 & 0 & 1.0000 & -0.0012 & 0.0387 & 0 & 0 \\ 0 & 0 & 0 & 0 & 0.9995 & 0.0301 & 0 & 0 \end{bmatrix}$$

$$\mathbf{B}_{25} = \begin{bmatrix} 2.8486 & -9.3393 & 1.6072 & 0.0000 \\ -0.5957 & -1.6601 & -10.1742 & 4.5635 \\ -97.2827 & -16.7355 & 0.1124 & -0.0000 \\ 8.1125 & -29.1930 & -155.4786 & -1.0327 \\ 5.5983 & 27.1773 & -5.2124 & -0.0854 \\ 12.1002 & -5.9431 & -27.3992 & -12.4912 \\ 0 & 0 & 0 & 0 \\ 0 & 0 & 0 & 0 \end{bmatrix}$$

$$\mathbf{A}_{50} = \begin{bmatrix} -0.0352 & 0.0012 & 0.0329 & -0.2390 & 1.1478 & 0.0000 & 0 & -9.8092 \\ 0.0047 & -0.0817 & -0.0174 & -1.2294 & -0.2224 & -49.4853 & 9.8055 & -0.0034 \\ -0.0065 & -0.0099 & -0.7845 & -0.5728 & 49.8288 & -0.0002 & 0.2692 & 0.1224 \\ 0.0012 & -0.1742 & 0.0439 & -10.4136 & -2.4104 & -0.0616 & 0 & 0 \\ 0.0223 & 0.0015 & -0.0342 & 0.4799 & -2.4287 & 0.0008 & 0 & 0 \\ -0.0199 & 0.1495 & -0.0208 & -1.7324 & -0.1675 & -1.3769 & 0 & 0 \\ 0 & 0 & 0 & 1.0000 & 0.0003 & -0.0125 & 0 & 0 \\ 0 & 0 & 0 & 0 & 0.9996 & 0.0274 & 0 & 0 \end{bmatrix}$$

$$\mathbf{B}_{50} = \begin{bmatrix} 0.9075 & -8.5200 & 1.5326 & 0.0000 \\ -1.5364 & -1.8060 & -10.1373 & 6.2898 \\ -121.0934 & -38.4155 & 0.1072 & 0.0000 \\ 11.9060 & -25.6546 & -155.2332 & -1.4233 \\ 13.7540 & 28.6606 & -5.2603 & -0.0574 \\ 11.1396 & -6.2134 & -26.9902 & -17.2165 \\ 0 & 0 & 0 & 0 \\ 0 & 0 & 0 & 0 \end{bmatrix}$$

$$\mathbf{A}_{70} = \begin{bmatrix} -0.0488 & 0.0010 & 0.0546 & -0.2673 & 5.4102 & 0.0000 & 0 & -9.7841 \\ 0.0067 & -0.1014 & -0.0237 & -5.5533 & -0.2358 & -69.1944 & 9.7748 & -0.0311 \\ 0.0092 & -0.0181 & -0.8310 & -0.8459 & 69.5240 & -0.0004 & 0.4279 & 0.7113 \\ -0.0085 & -0.2202 & 0.1040 & -9.9435 & -2.4907 & -0.0645 & 0 & 0 \\ 0.0287 & 0.0015 & -0.0457 & 0.5308 & -2.6444 & 0.0019 & 0 & 0 \\ -0.0295 & 0.1810 & 0.0372 & -1.6265 & -0.2122 & -1.6690 & 0 & 0 \\ 0 & 0 & 0 & 1.0000 & 0.0032 & -0.0727 & 0 & 0 \\ 0 & 0 & 0 & 0 & 0.9990 & 0.0437 & 0 & 0 \end{bmatrix}$$

$$\mathbf{B}_{70} = \begin{bmatrix} 1.2161 & -6.7805 & 0.8654 & 0.0000 \\ -1.9976 & -1.4391 & -10.3493 & 7.2563 \\ -133.0090 & -55.4407 & 0.0605 & -0.0000 \\ 21.1811 & -16.3533 & -156.0946 & -1.6420 \\ 20.2880 & 30.6086 & -4.9193 & -0.0698 \\ 18.6063 & -2.0112 & -27.2949 & -19.8620 \\ 0 & 0 & 0 & 0 \\ 0 & 0 & 0 & 0 \end{bmatrix}$$